





Deep learning-based signal-independent assessment of macular avascular area on 6×6 mm optical coherence tomography angiogram in diabetic retinopathy: a comparison to instrument-embedded software

Honglian Xiong,^{1,2} Qi Sheng You ,² Yukun Guo ,² Jie Wang,² Bingjie Wang,² Liqin Gao,² Christina J Flaxel,² Steven T Bailey ,² Thomas S Hwang,² Yali Jia ²

¹School of Physics and Optoelectronic Engineering, Foshan University, Foshan, Guangdong 528000, China
²Casey Eye Institute, Oregon Health & Science University, Portland, OR 97239, USA

Correspondence to

Dr Yali Jia, Casey Eye Institute, Oregon Health & Science University, Portland, OR 97239, USA; jiaya@ohsu.edu

Received 13 December 2020

Accepted 24 July 2021

Published Online First

13 September 2021

ABSTRACT

Synopsis A deep-learning-based macular extrafoveal avascular area (EAA) on a 6×6 mm optical coherence tomography (OCT) angiogram is less dependent on the signal strength and shadow artefacts, providing better diagnostic accuracy for diabetic retinopathy (DR) severity than the commercial software measured extrafoveal vessel density (EVD).

Aims To compare a deep-learning-based EAA to commercial output EVD in the diagnostic accuracy of determining DR severity levels from 6×6 mm OCT angiography (OCTA) scans.

Methods The 6×6 mm macular OCTA scans were acquired on one eye of each participant with a spectral-domain OCTA system. After excluding the central 1 mm diameter circle, the EAA on superficial vascular complex was measured with a deep-learning-based algorithm, and the EVD was obtained with commercial software.

Results The study included 34 healthy controls and 118 diabetic patients. EAA and EVD were highly correlated with DR severity ($p=0.812$ and -0.577 , respectively, both $p<0.001$) and visual acuity ($r=-0.357$ and 0.420 , respectively, both $p<0.001$). EAA had a significantly ($p<0.001$) higher correlation with DR severity than EVD. With the specificity at 95%, the sensitivities of EAA for differentiating diabetes mellitus (DM), DR and severe DR from control were 80.5%, 92.0% and 100.0%, respectively, significantly higher than those of EVD 11.9% ($p=0.001$), 13.6% ($p<0.001$) and 15.8% ($p<0.001$), respectively. EVD was significantly correlated with signal strength index (SSI) ($r=0.607$, $p<0.001$) and shadow area ($r=-0.530$, $p<0.001$), but EAA was not ($r=-0.044$, $p=0.805$ and $r=-0.046$, $p=0.796$, respectively). Adjustment of EVD with SSI and shadow area lowered sensitivities for detection of DM, DR and severe DR.

Conclusion Macular EAA on 6×6 mm OCTA measured with a deep learning-based algorithm is less dependent on the signal strength and shadow artefacts, and provides better diagnostic accuracy for DR severity than EVD measured with the instrument-embedded software.

characterised by microaneurysms, vascular permeability, ischaemia and neovascularisation.² Recent studies demonstrated that optical coherence tomography angiography (OCTA) is a promising tool for assessment of DR.^{3–24} Qualitative OCTA features of DR are well correlated with findings on fluorescein angiography.^{11 20} In addition, OCTA can provide objective quantitative metrics for retinal microangiopathy.²⁵ Studies demonstrated these OCTA metrics are correlated with disease severity.^{3–7 9 13–15 20 23}

The most commonly used quantitative OCTA parameter in DR is vessel density (VD), usually calculated as the number of pixels with flow signal divided by the area.^{3 24} This metric is widely adopted on commercial devices and many studies reported its relationship to DR severity and detection of vascular abnormalities in diabetics without clinically apparent retinopathy.^{4 7–9 12–14 22} However, VD measurements depend significantly on OCT signal strength.^{24 26–28} In contrast, our previous studies demonstrated that the avascular areas in 3×3 mm scans do not vary with signal strength while providing higher diagnostic accuracy for DR.²⁴

6×6 mm OCTA scans may improve diagnostic accuracy of DR severity level compared with 3×3 mm scans.^{3 29} However, compared with 3×3 mm, 6×6 mm scans are more prone to signal reduction artefacts caused by vignetting, vitreous floaters and defocus.³⁰ To account for the impact of signal reduction on vascular measurements on 6×6 mm scan, we have recently developed a deep learning-based method, named MEDnet, to distinguish true avascular area from OCTA signal loss due to signal reduction artefacts.^{30 31} We hypothesise that measurements that correctly compensate for signal reduction artefacts will correlate with clinical DR severity better than uncorrected measurements. In this study, we test the performance of MEDnet-detected 6×6 mm avascular area on diagnosing DR with different severities and compare its performance with VD measurements from commercially embedded software.

METHODS

The cross-sectional study recruited healthy participants and patients with diabetes from Oregon Health and Science University (OHSU).

INTRODUCTION

Diabetic retinopathy (DR) is a leading cause of vision loss worldwide in working age population,¹



© Author(s) (or their employer(s)) 2023. No commercial re-use. See rights and permissions. Published by BMJ.

To cite: Xiong H, You QS, Guo Y, et al. *Br J Ophthalmol* 2023;**107**:84–89.

Healthy participants and patients with type I diabetes of greater than 5 years duration or type II diabetes of any duration of age between 18 and 79 years were recruited. We excluded pregnant or lactating women for safety and practical reason since they were considered as vulnerable population in our studies, those unable to consent or cooperate with OCTA scans, or those with presence of significant non-diabetic ocular diseases or a history of intraocular surgery, except intravitreal injections or cataract surgeries, within 4 months prior to screening. One eye of each participant was included in the study. When two eyes were eligible for the study, the eye with a higher signal strength index (SSI) OCTA scans was selected.

All participants underwent a comprehensive clinical examination including systolic and diastolic blood pressure, protocol Early Treatment of Diabetic Retinopathy Study (ETDRS) visual acuity, intraocular pressure, axial length, slit-lamp biomicroscopy, indirect binocular funduscopy, ETDRS 7-field colour fundus photography and OCTA scans. A retinal specialist (TSH) determined the severity of DR based on standard 7-field ETDRS colour fundus photos using ETDRS severity scale masked to other clinical information and OCTA images.³²

6×6 mm OCTA scans centred on the fovea were acquired using a commercial 70 KHz spectral-domain OCT system (RTVue-XR; Optovue). Two repeated B-scans were taken at each of 400 raster positions and each B-scan consist of 400 A-lines. The OCTA data were computed using the split-spectrum amplitude decorrelation angiography algorithm.³³ The digital sampling interval was 20×20×3 µm/voxel. Two registered scans, 1 x-fast and 1 y-fast, were combined to form a single volume to reduce motion artefacts. We excluded scans with an SSI <55 or scan

quality index <6 or obvious residual motion artefacts. The automatically segmented upper and lower boundary of ganglion cell complex were manually reviewed and corrected when necessary. The maximum projection of flow signals within the inner 80% of ganglion cell complex generated superficial vascular complex (SVC) angiogram.^{24 34}

Our group recently developed and validated a custom deep-learning algorithm called MEDnet, which can detect avascular area on OCTA and differentiate from shadow area caused by signal reduction artefacts (figure 1). The details of the development of the algorithm have been reported previously.^{30 31} Briefly, the training data set was collected from 104 participants with a spectrum of DR severities (34 participants with diabetes without retinopathy, 31 participants with mild or moderate non-proliferative DR and 39 participants with severe DR) and 76 healthy controls. Sixfold cross-validation was adopted to evaluate the performance of MEDnet on the entire dataset. The ground truth maps for training were obtained by three certified graders manually delineated nonperfusion area (NPA) and signal reduction artefacts using in-house graphical user interface software. The input data set consisted of *en face* angiograms of the SVC, the inner retinal thickness map, the OCT reflectance image of the inner retina, and the corresponding manually delineated avascular area and the regions affected by signal reduction artefacts. MEDnet comprises three U-net like sub-convolution networks, enabling a stable training process while achieving high-resolution output.³¹ We modified the multi-scale module to enhance the feature representation capabilities of the network by making the network deeper. In each encoder and decoder block, we replaced plain connection blocks with residual blocks from

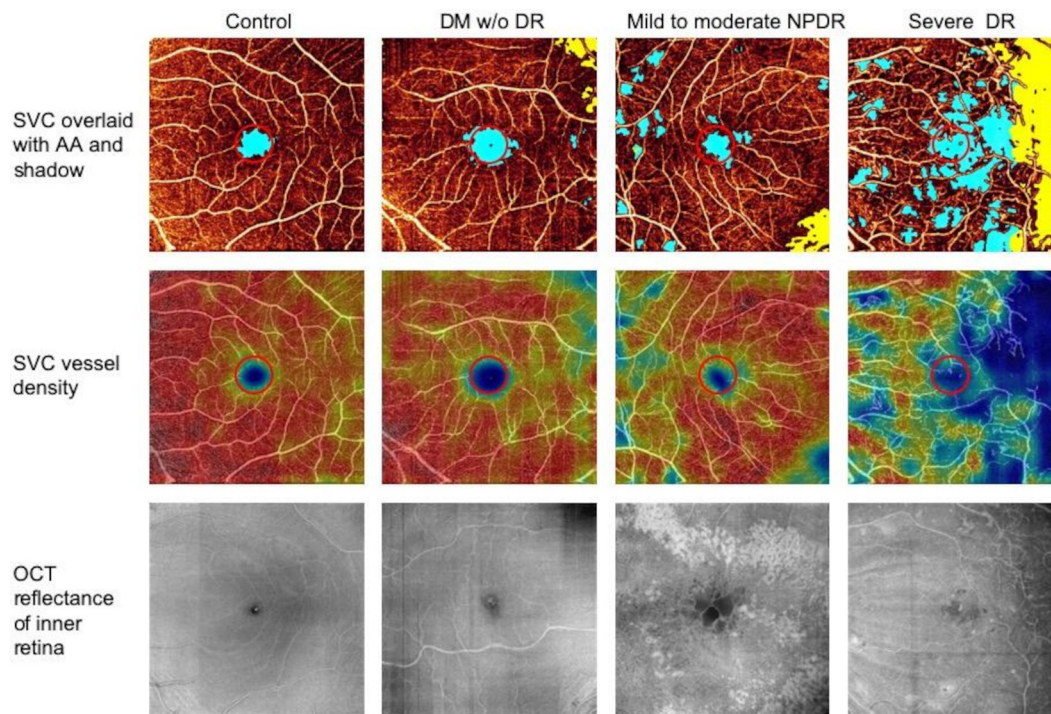


Figure 1 Avascular areas (AAs), shadow areas and vessel density map on 6×6 mm macular superficial vascular complex (SVC) angiograms of diabetic retinopathy with various severities. SVC overlaid with AA and shadow: in this SVC angiogram, AAs detected with MEDnet were labelled in blue and shadow artefacts were labelled in yellow. The central 1 mm red circle was excluded from analysis to avoid the impact of foveal avascular zone area. SVC vessel density: vessel density map output from the instrument-embedded commercial software. Note the peripheral blue regions show pseudo low vessel density due to shadow artefacts. Optical coherence tomography (OCT) reflectance of inner retina: *En face* OCT images of inner retinal slab (from inner limiting membrane to the lower boundary of outer plexiform layer). Shadow areas appear low reflectance. DM, diabetes mellitus; DR, diabetic retinopathy; NPDR, non-proliferative DR; w/o, without.

ResNet. The loss function was set as a weighted Jaccard loss to solve the category imbalance issue. The Adam algorithm with an initial learning rate of 0.001 was used as the optimiser. An early stopping strategy and a learning rate scheduler called reduce-learning-rate-on-plateau were applied in the training loop. After training, MEDnet can complete the analysis in less than 100 ms per case on a single central processing unit (CPU). The output of MEDnet shows high agreement (in pixels) with manual delineation of avascular area of all degrees of DR severity (Dice coefficient >0.82).³¹

The exact same version of the trained algorithm was used in the current study. The input images are OCT reflectance image of the inner retina, inner retinal thickness map and SVC angiogram, and the outputs are pixel classification (healthy retina, avascular area or shadow artefact). We excluded the central 1 mm diameter circle in our measurements to reduce the effect of normal variation in the foveal avascular zone size that may diminish the diagnostic accuracy,^{3 24 30 31} and measured the extrafoveal avascular area (EAA) on SVC. We also exported from device, measurements of VD on SVC from an instrument-embedded proprietary software—AngioAnalytics (V.2018.0.0.18). The VD outputs of AngioAnalytics include VD of whole scan region and foveal region (central 1 mm circle). To be consistent on analytic regions, the extrafoveal VD (EVD) was derived using the following formula:

$$EVD = \frac{VD_{overall} \times 6 \times 6 - VD_{foveal} \times \pi \times 0.5^2}{6 \times 6 - \pi \times 0.5^2}$$

All statistical analyses were performed using IBM SPSS for Windows (V.25.0, IBM SPSS). The Shapiro-Wilk test was used to evaluate normal distribution of all variables. Descriptive statistics included mean, SD, range and percentages were presented where appropriate. Analysis of variance was used to compare the EAA and EVD of different groups. Pearson correlation was used to analyse the associations between EAA, EVD, SSI, shadow area and best-corrected visual acuity (BCVA) or age. The association between DR severity and EAA, EVD or other quantified parameters was analysed using Spearman correlation. Z-test was used to compare the correlation coefficients. Pearson correlation and linear regression analysis were used to analyse the dependence of EAA or EVD on clinical covariates such as age, axial length, SSI and shadow area. The area under the receiver-operating curve (AOC) and the corresponding sensitivity at 95% specificity were calculated to assess the diagnostic accuracy of EAA or EVD for differentiating DM, DR or severe DR from control.

The Delong method was used to compare the AOCs. The McNemar test was used to compare sensitivities. All p values were two-sided and considered statistically significant if the value was less than 0.05.

RESULTS

The study included 152 participants (63 male, 41.4%) with a mean age of 54 years, including 34 healthy controls, 30 patients with diabetes without DR, 31 patients with mild to moderate non-proliferative diabetic retinopathy (NPDR) and 57 patients with severe DR (severe NPDR or proliferative DR). The demographic and clinical characteristics of the participants were summarised in table 1.

The mean SVC EAA significantly increased with severity of DR while the mean SVC VD significantly decreased with severity of DR (figure 1 and table 2). Both EAA and EVD were highly correlated with DR severity ($p=0.812$ and -0.577 for EAA and EVD, respectively, both $p<0.001$) and BCVA ($r=-0.357$ and 0.420 for EAA and EVD, respectively, both $p<0.001$). EAA had significantly ($p<0.001$) higher correlations with DR stage than EVD.

EAA had a greater AOC than EVD (0.907 vs 0.858, $p=0.26$) for differentiating DM from control, but this difference was not statistically significant. For differentiating DR (0.974 vs 0.883, $p=0.02$) or severe DR (1.000 vs 0.906, $p=0.01$) from control, EAA had significantly greater AOCs than EVD (figure 2). When the specificity was fixed at 95%, EAA had a significantly higher sensitivity than EVD for detection of DM (80.5% vs 11.9%, $p=0.001$), any DR (92.0% vs 13.6%, $p<0.001$) or severe DR (100.0% vs 15.8%, $p<0.001$) from control.

We found EVD was significantly confounded by factors at scan acquisition level (figure 3). In healthy control group, EVD was significantly associated with SSI ($r=0.434$, $p=0.01$) and shadow area ($r=-0.478$, $p=0.004$), but was not significantly associated with age ($r=-0.199$, $p=0.26$) or axial length ($r=0.006$, $p=0.97$). On the contrary, the EAA was not significantly associated with SSI ($r=-0.044$, $p=0.805$), shadow area ($r=-0.046$, $p=0.796$), age ($r=0.128$, $p=0.471$) or axial length ($r=0.140$, $p=0.431$). Shadow areas measured by MEDnet were highly correlated with SSI ($r=-0.665$, $p<0.001$), an indicator of scan quality on AngioVue.

For the overall study groups, the SSI ($r=-0.451$, $p<0.001$) and shadow area ($r=0.291$, $p<0.001$) were highly correlated with age. Both factors were significantly associated with DR

Table 1 Demographic and clinical characteristics of the study participants

Characteristic	Control (n=34)	DM w/o DR (n=30)	Mild to moderate NPDR (n=31)	Severe DR (n=57)
Age, year, mean (SD)	40.6 (15.9)	55.4 (15.3)	64.0 (11.3)	56.4 (14.3)
Female, N (%)	20 (58.8)	17 (56.7)	19 (61.3)	33 (57.9)
Type 1 DM, N (%)	NA	4 (13.3)	8 (25.8)	18 (31.5)
HbA1c, %, mean (SD)	NA	7.45 (1.54)	7.39 (1.02)	8.25 (1.94)
DM duration, year, mean (SD)	NA	11.9 (11.2)	24.7 (15.2)	22.8 (11.0)
SBP, mm Hg, mean (SD)	114.2 (13.4)	129.4 (18.0)	132.3 (16.0)	135.7 (23.6)
DBP, mm Hg, mean (SD)	71.1 (13.4)	77.3 (13.2)	69.2 (12.4)	76.3 (14.9)
Prevalence of DME, No. (%)	NA	0 (0)	17 (57)	44 (77)
BCVA, ETDRS letters, mean (SD)	88.7 (4.2)	81.7 (7.7)	76.9 (9.7)	79.1 (6.6)
IOP, mm Hg, mean (SD)	13.9 (3.0)	15.7 (3.6)	15.9 (3.3)	14.0 (3.3)
Axial length, mm, mean (SD)	23.9 (1.0)	23.9 (1.0)	23.6 (0.7)	23.6 (1.0)
BCVA, best-corrected visual acuity; DBP, diastolic blood pressure; DM, diabetes mellitus; DME, diabetic macular oedema; DR, diabetic retinopathy; ETDRS, Early Treatment Diabetic Retinopathy Study; HbA1c, glycated haemoglobin; IOP, intraocular pressure; NA, not applicable; NPDR, non-proliferative diabetic retinopathy; SBP, systolic blood pressure; severe DR, severe non-proliferative diabetic retinopathy or proliferative diabetic retinopathy.				

Table 2 Measurements on 6×6 mm macular superficial vascular complex angiograms of diabetic retinopathy with various severities

Measurements mean (SD)	Control (n=34)	DM w/o DR (n=30)	Mild to moderate DR (n=31)	Severe DR (n=57)	P value
EAA (mm ²)	0.110 (0.087)	0.340 (0.534)	1.008 (0.995)	1.953 (1.175)	<0.001
EVD (% area)	52.0 (4.4)	47.8 (5.2)	46.7 (5.0)	43.9 (5.4)	<0.001
SSI	75.7 (5.5)	68.1 (6.9)	64.2 (7.4)	64.2 (5.3)	<0.001
Shadow area (mm ²)	1.138 (1.122)	2.066 (2.405)	2.460 (1.680)	2.621 (2.090)	0.004

P value was acquired by analysis of variance.

DM w/o DR, diabetes without diabetic retinopathy; EAA, extrafoveal avascular area; EVD, extrafoveal vessel density; severe DR, severe non-proliferative diabetic retinopathy or proliferative diabetic retinopathy; SSI, signal strength index.

stage ($p=0.335$ and -0.531 for shadow area and SSI, respectively, both $p<0.001$) and visual acuity ($r=-0.238$, $p=0.003$ and $r=0.478$, $p<0.001$ for shadow area and SSI, respectively).

The associations between SSI or shadow area and EVD, SSI or shadow area and disease severity, suggested the necessity of adjustment of EVD with SSI and shadow area. After adjustment with these covariates using multivariate linear regression model, the diagnostic accuracy of EVD for differentiating different severity of DR from control significantly decreased (figure 2A-C). The AROCs of adjusted EVD were significantly lower than those of unadjusted EVD for differentiating DM from control (0.746 vs 0.858, $p=0.006$) and differentiating DR from control (0.765 vs 0.883, $p=0.003$), lower but not significant for differentiating severe DR from control (0.849 vs 0.909, $p=0.135$). The AROCs of adjusted EVD was significantly lower than that of EAA for detection of DM ($p=0.002$), DR ($p<0.001$) or severe DR ($p=0.001$).

DISCUSSION

This study demonstrated that a deep learning-based measurement of avascular area on SVC provided a superior diagnostic accuracy compared with commercial VD measurements in DR. The high sensitivities in detecting DR (92.0%) and severe DR (100%) at a high specificity (95%) suggest the deep-learning based avascular area measurement may be useful in assisting clinicians to accurately assess DR severity. The algorithm may also be useful in automated DR screening using OCTA. In clinical assessment scenario, we fix specificity at 95% to limit false positive cases, so to avoid unneeded further examination or treatment. For screening purpose, a higher specificity could limit false positive cases to avoid unneeded referral and reduce burden

to healthcare system. However, to reduce missed case, a higher sensitivity with trade-off specificity is preferred.

The superiority of the deep learning-based measurement of avascular area can be explained by the difference in the nature of the biomarkers and the importance of addressing signal reduction artefacts. First, VD measures perfusion (flow pixels), while avascular area measures non-perfusion (non-flow pixels). In the simplest model, within the same region of interest (ROI), they are linearly related by the formula $1=VD+AA/ROI$. However, the OCTA flow pixels may be more vulnerable to low OCT signal strength caused by beam attenuation and beam aberration than non-flow pixels. For instance, we frequently see the disconnected and disappeared vasculatures on OCT angiograms due to media opacity (eg, cataract, vitreous floaters), and artifactually thickened vasculatures due to defocus or astigmatism. However, the algorithm limits the detected the avascular areas by a minimum continuous areas of non-flow pixels, decreasing the probability that low signal artefacts contribute to the measurement. Therefore, the analysis based on flow pixels is expected to be more dependent on SSI (figure 3) than the analysis based on non-flow pixels.

Second, signal reduction artefacts on OCTA, particularly severe ones caused by pupil vignetting, large floaters or severe defocus have a significant impact on the measurement accuracy.²⁶ Using manual correction of shadow areas,³⁵ De Pretto also demonstrated that the removal of shadow area is imperative to measuring retinal circulation. By taking advantage of a deep convolution neural network trained to distinguish non-flow pixels into avascular area versus shadow area, we were able to improve the accuracy of the measurements (figure 2).

Using macular 6×6 mm scans from healthy controls, we demonstrated that avascular area measurements are independent of SSI and

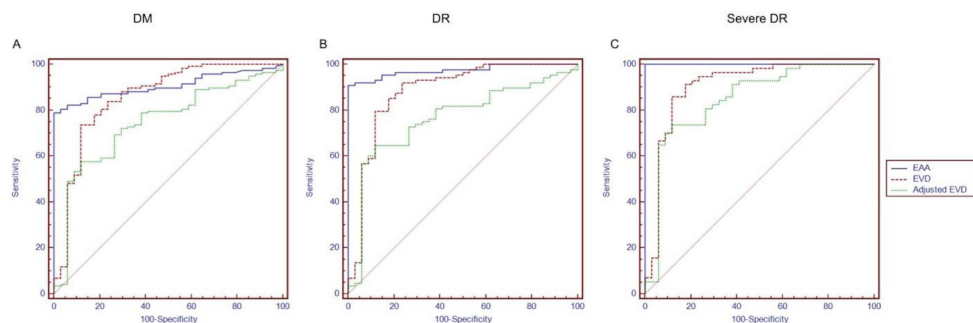


Figure 2 The diagnostic accuracy of extrafoveal avascular area, extrafoveal vessel density and adjusted extrafoveal vessel density for differentiating diabetic retinopathy severities from control. The EAA (measured with a deep learning-based algorithm) shows a slightly but not significant greater area under the receiver operating characteristic curve (AOC) than EVD (measured with the instrument-embedded commercial software) for differentiating DM from control. For differentiating DR or severe DR from control, EAA had significantly greater AOCs than EVD. The AOCs of adjusted EVD (with signal strength index (SSI) and shadow area) are significantly lower than those of EAA for detection of DM, DR or severe DR. Adjusted EVD, EVD adjusted with age and SSI; DM, diabetes mellitus; DR, diabetic retinopathy; EAA, extrafoveal avascular area; EVD, extrafoveal vessel density; severe DR, severe non-proliferative diabetic retinopathy or proliferative diabetic retinopathy.

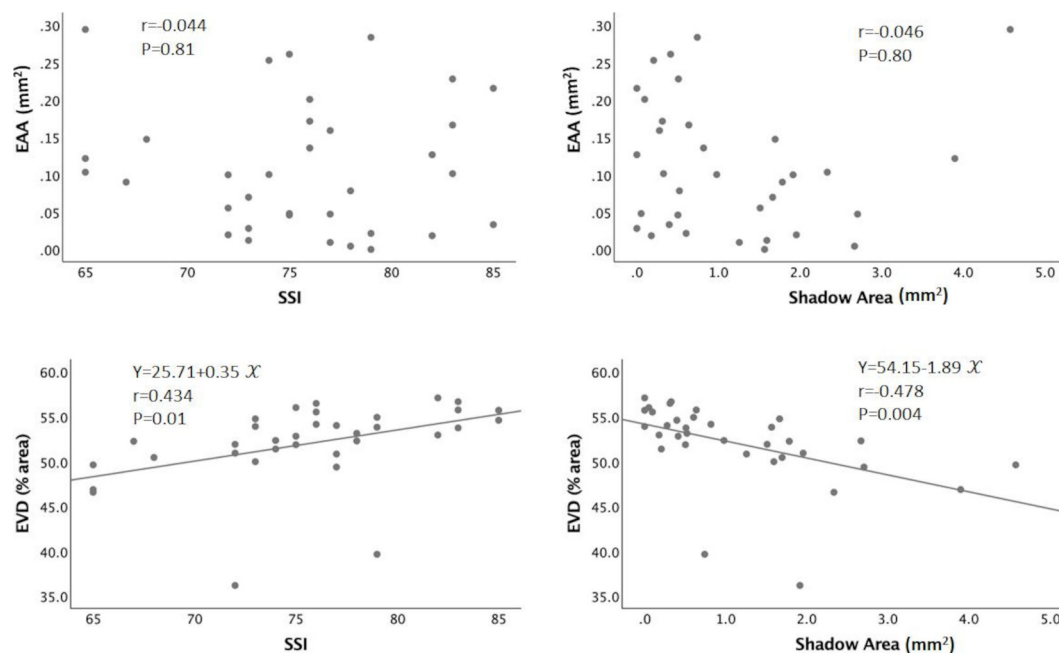


Figure 3 Effects of scan quality on vascular measurements in healthy controls. The upper panel demonstrates EAA measured with our custom deep-learning software is independent from SSI and shadow area. The low panel demonstrates EVD measured with instrument-embedded commercial software significantly increases with SSI and decreases with shadow area. EAA, extrafoveal avascular area; EVD, extrafoveal vessel density; SSI, signal strength index.

shadow area, while the commercial VD measurements are linearly related to SSI and shadow area. The dependency of VD on SSI is consistent with the previous finding on 3×3 mm scans.²⁴ SSI and shadow area are simply different metrics of scan quality that indicate the impacts of OCT beam attenuation and aberration. SSI is a measurement based on the average tissue reflectance amplitude on the OCT image on a logarithmic scale. Thus, a negative relationship between SSI and shadow area is expected. This also further validates the detection accuracy of shadow area by MEDnet.

This study found a direct relationship between scan quality and DR severity. While the relationship is weaker than actual microvascular changes seen on OCTA, a reduction in SSI and an increase in shadow areas are associated with worsening DR severity, worse visual acuity and increasing age. This could be explained by an increased probability of cataract, vitreous floaters and poor tear film quality with worse disease that contribute to low signal artefacts. Therefore, without accounting for scan quality effects, previous studies may have overestimated the rate of VD decline with DR stage, vision and age.

It is interesting to note that the confounding effect on EVD led to a low sensitivity at high specificity and false high sensitivity at low specificity. This was particularly true in early stage disease, as illustrated in figure 2A. After adjustment of EVD with SSI and shadow area, the AROCs of EVD decreased mainly due to the removal of artificial detection of DR with low-quality scans, but adjusted EVD shows improved sensitivity at high specificity. This suggests that without compensating for these confounding factors, one can arrive at an erroneous conclusion about the significance of the vascular parameters.

Finally, we should note that 6×6 mm OCTA scan is more susceptible to signal reduction artefacts (figure 1) than 3×3 mm scans, and the scan quality is in general, more variable in DR and non-DR populations. Even with some quality control suggested by OCTA manufacturers, the acceptable scans still span a wide range in signal strength. Thus, appropriate compensation for signal strength

variation using tools like artificial intelligence is even more critical when evaluating wider-field OCTAs for vascular metrics.

Limitations of the current study have to be acknowledged. First, we only measured the EAA and EVD on SVC, but not on deeper retinal layers, for we only trained the deep learning algorithm on SVC. The advantage of measuring EAA and EVD on SVC only is that we can reduce the impact of macular oedema on the measurement. Second, we excluded scans with an SSI <55 and scan quality index <6 or obvious residual motion artefacts in this study. These low-quality scans carry many types of artefacts due to the failure of instrument-embedded registration software, so the detection of avascular area based on these scans are meaningless, which will jeopardise the comparison in this study. Deep learning method alone cannot magically wipe off the problem produced by the data acquisition steps, but deep learning approaches and upstream steps can work synergistically to improve the data readability. Third, our sample size is relatively small. We have to combined mild and moderate NPDR into one group, and severe NPDR and PDR into one group when performing statistical analysis.

In summary, a deep learning-based algorithm can reduce the impact of signal reduction artefacts and objectively measure macular avascular area caused by DR. Compared with the commonly available commercial metrics such as VD, EAA measured with the deep learning algorithm has a significant higher sensitivity for differentiating DR severity. This approach may be more useful for assessment of DR, especially when a wider field scan is used.

Twitter Bingjie Wang @BingjieWang_CEI

Contributors Concept and design: HX, QY, YJ. Acquisition, analysis, or interpretation of data: HX, QY, YG, BW, JW, CJF, STB, TSH. Drafting of the manuscript: HX, QY, YJ. Critical revision of the manuscript for important intellectual content: all authors. Statistical analysis: HX, QY. Administrative, technical or material support: YJ, JW, BW, YG. Supervision: YJ. YJ had full access to all the data in the study and takes responsibility for the integrity of the data and the accuracy of the data analysis.

Funding The study was supported by grants R01 EY027833, R01 EY024544 and P30 EY010572 from the National Institutes of Health, an unrestricted departmental funding grant, and William & Mary Greve Special Scholar Award from Research to Prevent Blindness, New York. The sponsor or funding organisation had no role in the design, conduct or submission of this research.

Competing interests YJ and STB (financial support) have a significant financial interest in Optovue Inc. These potential conflicts of interest have been reviewed and are managed by OHSU. The other authors do not have any potential financial conflicts of interest.

Patient consent for publication Obtained.

Ethics approval The study protocol was performed in compliance with the Declaration of Helsinki and approved by the institutional review board of OHSU. All the participants provide informed written consent.

Provenance and peer review Not commissioned; externally peer reviewed.

Data availability statement Data are available upon reasonable request. All data relevant to the study are included in the article or uploaded as supplementary information. None.

ORCID iDs

Qi Sheng You <http://orcid.org/0000-0003-0743-7320>

Yukun Guo <http://orcid.org/0000-0002-6784-2355>

Steven T Bailey <http://orcid.org/0000-0003-4949-1464>

Yali Jia <http://orcid.org/0000-0002-2784-1905>

REFERENCES

- Bourne RRA, Stevens GA, White RA, *et al.* Causes of vision loss worldwide, 1990–2010: a systematic analysis. *Lancet Glob Health* 2013;1:e339–49.
- Antonetti DA, Klein R, Gardner TW. Diabetic retinopathy. *N Engl J Med* 2012;366:1227–39.
- Hwang TS, Gao SS, Liu L, *et al.* Automated quantification of capillary nonperfusion using optical coherence tomography angiography in diabetic retinopathy. *JAMA Ophthalmol* 2016;134:367–73.
- Ashraf M, Nesper PL, Jampol LM, *et al.* Statistical model of optical coherence tomography angiography parameters that correlate with severity of diabetic retinopathy. *Invest Ophthalmol Vis Sci* 2018;59:4292–8.
- Bhanushali D, Anegondi N, Gadde SGK, *et al.* Linking retinal microvasculature features with severity of diabetic retinopathy using optical coherence tomography angiography. *Invest Ophthalmol Vis Sci* 2016;57:OCT519–25.
- Bhardwaj S, Tsui E, Zahid S, *et al.* Value of fractal analysis of optical coherence tomography angiography in various stages of diabetic retinopathy. *Retina* 2018;38:1816–23.
- Binotti WW, Romano AC. Projection-resolved optical coherence tomography angiography parameters to determine severity in diabetic retinopathy. *Invest Ophthalmol Vis Sci* 2019;60:1321–7.
- Dimitrova G, Chihara E, Takahashi H, *et al.* Quantitative retinal optical coherence tomography angiography in patients with diabetes without diabetic retinopathy. *Invest Ophthalmol Vis Sci* 2017;58:190–6.
- Durbin MK, An L, Shemonski ND, *et al.* Quantification of retinal microvascular density in optical coherence tomographic angiography images in diabetic retinopathy. *JAMA Ophthalmol* 2017;135:370–6.
- Fawzi AA, Fayed AE, Linsenmeier RA, *et al.* Improved macular capillary flow on optical coherence tomography angiography after panretinal photocoagulation for proliferative diabetic retinopathy. *Am J Ophthalmol* 2019;206:217–27.
- Hwang TS, Jia Y, Gao SS, *et al.* Optical coherence tomography angiography features of diabetic retinopathy. *Retina* 2015;35:2371–6.
- Kaizu Y, Nakao S, Sekiryu H, *et al.* Retinal flow density by optical coherence tomography angiography is useful for detection of nonperfused areas in diabetic retinopathy. *Graefes Arch Clin Exp Ophthalmol* 2018;256:2275–82.
- Kim AY, Chu Z, Shahidzadeh A, *et al.* Quantifying microvascular density and morphology in diabetic retinopathy using spectral-domain optical coherence tomography angiography. *Invest Ophthalmol Vis Sci* 2016;57:OCT362–70.
- Lee H, Lee M, Chung H, *et al.* Quantification of retinal vessel tortuosity in diabetic retinopathy using optical coherence tomography angiography. *Retina* 2018;38:976–85.
- Lu Y, Simonett JM, Wang J, *et al.* Evaluation of automatically quantified foveal avascular zone metrics for diagnosis of diabetic retinopathy using optical coherence tomography angiography. *Invest Ophthalmol Vis Sci* 2018;59:2212–21.
- Motulsky EH, Liu G, Shi Y, *et al.* Widefield swept-source optical coherence tomography angiography of proliferative diabetic retinopathy. *Ophthalmic Surg Lasers Imaging Retina* 2019;50:474–84.
- Pan J, Chen D, Yang X, *et al.* Characteristics of neovascularization in early stages of proliferative diabetic retinopathy by optical coherence tomography angiography. *Am J Ophthalmol* 2018;192:146–56.
- Rosen RB, Andrade Romo JS, Krawitz BD, *et al.* Earliest evidence of prediabetic retinopathy revealed using optical coherence tomography angiography perfused capillary density. *Am J Ophthalmol* 2019;203:103–15.
- Sandhu HS, Eladawi N, Elmogy M, *et al.* Automated diabetic retinopathy detection using optical coherence tomography angiography: a pilot study. *Br J Ophthalmol* 2018;102:1564–9.
- Soares M, Neves C, Marques IP, *et al.* Comparison of diabetic retinopathy classification using fluorescein angiography and optical coherence tomography angiography. *Br J Ophthalmol* 2017;101:62–8.
- Spaide RF. Volume-rendered angiographic and structural optical coherence tomography. *Retina* 2015;35:2181–7.
- Tang F, Cheung CY. Quantitative retinal optical coherence tomography angiography in patients with diabetes without diabetic retinopathy. *Invest Ophthalmol Vis Sci* 2017;58:1766.
- Tang FY, Ng DS, Lam A, *et al.* Determinants of quantitative optical coherence tomography angiography metrics in patients with diabetes. *Sci Rep* 2017;7:2575.
- Hwang TS, Hagag AM, Wang J, *et al.* Automated quantification of nonperfusion areas in 3 vascular plexuses with optical coherence tomography angiography in eyes of patients with diabetes. *JAMA Ophthalmol* 2018;136:929–36.
- Spaide RF, Fujimoto JG, Waheed NK, *et al.* Optical coherence tomography angiography. *Prog Retin Eye Res* 2018;64:1–55.
- Gao SS, Jia Y, Liu L, *et al.* Compensation for reflectance variation in vessel density quantification by optical coherence tomography angiography. *Invest Ophthalmol Vis Sci* 2016;57:4485–92.
- You QS, Chan JCH, Ng ALK, *et al.* Macular vessel density measured with optical coherence tomography angiography and its associations in a large population-based study. *Invest Ophthalmol Vis Sci* 2019;60:4830–7.
- Lim HB, Kim YW, Nam KY, *et al.* Signal strength as an important factor in the analysis of peripapillary microvascular density using optical coherence tomography angiography. *Sci Rep* 2019;9:16299.
- Tan B, Chua J, Lin E, *et al.* Quantitative microvascular analysis with wide-field optical coherence tomography angiography in eyes with diabetic retinopathy. *JAMA Netw Open* 2020;3:e1919469.
- Guo Y, Camino A, Wang J, *et al.* MEDnet, a neural network for automated detection of avascular area in OCT angiography. *Biomed Opt Express* 2018;9:5147–58.
- Guo Y, Hormel TT, Xiong H, *et al.* Development and validation of a deep learning algorithm for distinguishing the nonperfusion area from signal reduction artifacts on OCT angiography. *Biomed Opt Express* 2019;10:3257–68.
- Grading diabetic retinopathy from stereoscopic color fundus photographs--an extension of the modified airline house classification. ETDRS report number 10. early treatment diabetic retinopathy study research group. *Ophthalmology* 1991;98:786–806.
- Jia Y, Tan O, Tokayer J, *et al.* Split-spectrum amplitude-decorrelation angiography with optical coherence tomography. *Opt Express* 2012;20:4710–25.
- Campbell JP, Zhang M, Hwang TS, *et al.* Detailed vascular anatomy of the human retina by projection-resolved optical coherence tomography angiography. *Sci Rep* 2017;7:42201.
- De Pretto LR, Moulton EM, Alibhai AY, *et al.* Controlling for artifacts in widefield optical coherence tomography angiography measurements of non-perfusion area. *Sci Rep* 2019;9:9096.